

The Structural, Dielectric and AC Conductivity Studies of TiCo Substituted Sr₂NiZn Y-Type Hexa Nanoferrites

Vijay V. Warhate¹, Dilip S. Badwaik²

^aS.N Mor College, Tumsar, India-441912

^bKamla Nehru College, Nagpur, India-440009

Abstract: In the present investigation we synthesized a series of polycrystalline Y-type SrNiZn nano hexa ferrites substituted with TiCo having generic formula Sr₂NiZnFe_{12-x}(TiCo)_{x/2}O₂₂ (where x = 0.0, 0.5, 1.0, 1.5) by novel microwave assisted sol-gel auto combustion route. Structural analysis of the compounds has been studied using X-ray powder diffraction pattern. The prepared compounds are in single Y-type hexagonal phase with the space group R $\bar{3}m$ (no. 166). The lattice parameters, experimental density, X-ray density and porosities of compounds were measured from XRD data. It is observed that the lattice parameter "a" is almost remains constant and easy magnetized "c" axis undergoes more expansion with content of TiCo. The average grain size of the prepared samples measured from Scherer formula is in nanometer range. The frequency dependant ac electrical conductivity, dielectric constant and dielectric loss were measured at room temperature in the range 100Hz- 0.2 MHz. The phenomenon of dielectric dispersion in ferrites has been explained on the basis of Maxwell-Wagner model and Koop's phenomenological theory of dielectric.

Keywords: Y-type nano hexaferrites, X-ray Diffraction, Dielectric constant, AC conductivity

1. Introduction

Today ceramic magnetic materials, capable of combining a high resistivity and a high permeability, are found in numerous products used in our everyday life. They play a very important role in various technological applications such as microwave devices, high speed recording media, ferrofluids, catalysis and magnetic refrigeration systems¹. Ferrimagnetic nanocrystallites are of particular interest because they can exhibit a single magnetic domain. The electrical and dielectric properties of the hexaferrites can be tailored to specific device applications by choice of different cations and cation distribution between interstitial sites. Method of preparation, sintering temperature, sintering time and preparation condition are also important parameters that affect properties of hexaferrites². The magnetic properties of hexaferrites³, d c electrical conductivity and thermoelectric power of Y-type hexaferrites⁴, the dielectric properties and ac conductivity of W-type and M-type^{5, 6} have been extensively studied. The ac conductivity of ferrites gives valuable information related to the localization of charge carriers at grain and grain boundaries, inter-granular tunnelling of charge carriers across the grain boundary and dielectric polarization of magnetic ions^{7,8}.

The crystal structure of Y-type hexaferrites consist of basic units of hexagonal M ferrite and cubic spinel ferrites that retain a hexagonal crystal structure usually with direction of magnetization parallel to c- axis. Y-type hexaferrites consider as interesting and promising high frequency material, because of their very usefulness in VHF and UHF.

In the present paper, we synthesized Y-type nanohexaferrites with generic formula Sr₂NiZnFe_{12-x}(TiCo)_{x/2}O₂₂ where x= 0, 0.5, 1.0 & 1.5 by microwave assisted sol-gel auto combustion route from metal nitrates and urea as a precursor. The synthesized samples were

characterized by XRD, a c electrical conductivity (σ), dielectric constant (ϵ') and dielectric tangent loss ($\tan\delta$).

2. Experimental Procedure

2.1 Synthesis Technique

TiCo substituted Sr₂NiZn -ferrite having empirical formula Sr₂NiZnFe_{12-x}(TiCo)_{x/2}O₂₂ where x = 0 to 1.5 in equal steps of 0.5 were prepared by microwave assisted sol gel combustion method. The starting chemicals used were AR grade strontium nitrate, iron nitrate, zinc nitrate, nickel Nitrate, cobalt nitrate, titanium chloride where used as starting oxidizing material and urea is used as reducing agent to supply requisite energy to initiate exothermic reaction amongst oxidants. Stoichiometric amount of starting materials and fuel were dissolved one by one in 30 ml of triple distilled water to prepare a solution, to which urea was added. It is then heated with continuous stirring at 95 °C to form gel. The beaker containing gel was kept in a domestic microwave oven and was irradiated with microwaves. After few minutes dark brown fumes started coming out and gel solution fired into flames and resulted into a foamy dark brown powder. The synthesized compounds were milled in a pestle mortar for about one hour, then calcinated at 900 °C for about five hour in furnace and cooled to room temperature by natural way. The calcinated powder again milled for 1 hour to get fine powder of Y-type nano hexaferrites.

2.2 Sample Characterizations

The structure was determined through the X-ray diffraction (XRD) analysis. XRD patterns were taken using Cu K α (λ = 1.5406 Å) radiation at room temperature. The average crystallite size, lattice parameter, bulk density, X-ray density and porosity were calculated using simple formulae⁹. For

dielectric measurement, pellets were made using dye punch of 10mm diameter and applying a pressure of 6.5 kN using hydraulic press. The dielectric measurements were carried out at room temperature in the frequency range 100Hz-200kHz by the LCR-Q meter (Model Hemeg 8118).

3. Results and Discussion

3.1 Structural Analysis

Structural analysis of all TiCo substituted Sr_2NiZnY -type hexaferrite compounds under investigation were performed by X-ray diffraction pattern shown in Fig. 1. The values of molecular weight(M), lattice parameters (a and c), cell volume, experimental density D (the bulk density), X-ray density D_x (the theoretical density) and porosity(P) of all the compounds are enumerated in Table 1 for the purpose of consolidation and overall comparative view.

The crystallographic results of these compounds reveal that, they are Y-type hexagonal ferrite and most of the peaks matched with standard XRD pattern of Y-type hexa ferrite. All the compounds belong to the $R\bar{3}m$ (no.166) space group. It is observed that the lattice parameter "a" is almost remains constant and easy magnetized "c" axis undergoes more expansion with content of TiCo. This increase in the lattice parameter "c" can be explained on the basis of the ionic radii. The ionic radii of the Ti^{+4} ion is (0.74 Å) and Co^{2+} ion is (0.72 Å). Since the ionic radius of Ti^{+4} and Co^{2+} is more than that of Fe^{3+} (0.64 Å), the increase in lattice parameters with TiCo substitution is expected. It is also shown that the values of the lattice parameters are in satisfactory agreement with the published results for Y-type hexagonal ferrites¹⁰, where $a=5.86\text{Å}$ and $c=42.47\text{Å}$. The value of x-ray density for all compounds are compatible with that reported in the literature i.e. 5.2 gm/cm^3 .¹¹

However, the experimental density D values were found to be much smaller than the X-ray density D_x , indicating that prepared compounds are highly porous materials. Table.1 shows a decrease in the bulk density and a corresponding increase in porosity P with increase in content of Ti, Co ions. This behaviour

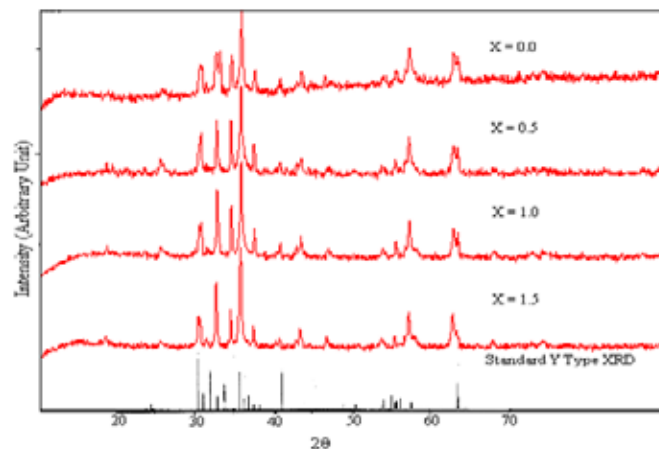


Fig-1. XRD Spectra of $Sr_2NiZnFe_{12-x}(TiCo)_{x/2}O_{22}$

may be attributed to the fact that the introduction of Ti, Co ions in hexaferrite affects the grain size development during sintering.

The XRD pattern is also used to calculate the grain size of the prepared compounds. Grain size of all the compounds is calculated from most intense peak using Scherer formula.

$$D = 0.9\lambda / \beta \cos\theta$$

Where, λ is the wavelength.

β is the full width at half maxima (FWHM).

θ is the corresponding position at particular angle.

The crystallite size calculated is found to be in range of 30 nm to 82 nm.

Table 1: Molecular weight, Lattice constants (a, c), cell volume (v), X-ray density (D_x), Bulk density (D), Porosity (P), of $Sr_2NiZnFe_{12-x}(TiCo)_{x/2}O_{22}$

Compounds	Mol. Wt.	Lattice Parameter		Cell Vol. (Å^3)	D_x g/cc	D g/cc	Porosity (P) %	Grain Size nm (XRD)
		a (Å)	c(Å)					
X = 0	1321.45	5.8688	42.4725	1266.88	5.1954	3.5479	31.71	30.93
X = 0.5	1320.22	5.8490	42.5597	1260.82	5.2155	3.4222	34.38	70.70
X= 1.0	1319.00	5.8436	42.4628	1255.74	5.2318	3.6614	30.01	70.36
X= 1.5	1317.78	5.8621	42.6649	1269.71	5.1694	3.7181	28.07	82.43

3.3 Dielectric Studies

Dielectric constant (ϵ') in ferrites is contributed by several structural and micro-structural factors. The variation of dielectric constant with frequency at room temperature is shown in Fig.2. It is observed that dielectric constant decreases rapidly in low frequency region and slows down in high frequency region, almost approaches to frequency independent behaviour. The phenomenon of dielectric dispersion in ferrites has been explained on the basis of Maxwell-Wagner model¹² and Koop's phenomenological theory¹³ of dielectric. This model, suggests that dielectric medium is made of well conducting grains, separated by poorly conducting grain boundaries. It has been observed that in ferrites the dielectric constant is directly proportional to the square root of conductivity¹⁴. Therefore the grains are highly conductive and have high value of dielectric constant,

while as the grain boundaries are less conductive and have smaller values of dielectric constant. At lower frequencies the grains are more effective than grain boundaries in electrical conduction. Thinner the grain boundary, higher is the value of dielectric constant. The higher values of the dielectric constant observed at lower frequencies are also explained on the basis of interfacial / space polarization due to inhomogeneous dielectric structure¹⁵. The inhomogeneities present in the system can be porosity and grain structure. The maximum value of ϵ' is found for X=1.0

Fig.3 shows the behaviour of dielectric loss as a function of frequency for all compounds at room temperature. The dielectric loss is defined as the ratio of loss or resistive current to the charging current in the compounds. The relaxation peak is observed for sample X=0.5 at a frequency of 6 kHz. There may be relaxation peaks for other samples

too in the lower frequency side less than 1 kHz. The appearance of relaxation peak can be explained according to Debye relaxation theory¹⁶. The loss peak occurs when the applied field is in phase with the dielectric and the condition $\omega\tau = 1$ is satisfied, where $\omega=2\pi f$, f being the frequency of applied field. Similar results of maxima have been reported in the dielectric loss versus frequency graph for SrNiZn Y-type ferrites¹⁷.

3.4 AC Conductivity

The frequency dependence of ac conductivity ($\log \bar{\sigma}_{ac}$) for different concentration of Ti^{+4} and Co^{2+} ($X=0, 0.5, 1.0, 1.5$) measured at room temperature is shown in Fig 4. All the samples show a normal ferromagnetic behaviour. It is observed that conductivity increases with increase in frequency for all prepared compounds. The conduction mechanism in ferrites is explained on the basis of hopping of charge carriers between the Fe^{2+} and Fe^{3+} ions on octahedral site.

The increase in frequency enhances the hopping frequency of charge carriers resulting in an increase in the conduction process thereby increasing the conductivity. Ferrites are low mobility materials and the increase in conductivity does not mean that the number of charge carriers increases, but only the mobility of carriers. The number of ferrous (Fe^{2+}) ions play a dominant role in the mechanism of conduction and dielectric polarization. The presence of small amount of Fe^{2+} ions increases electrical conductivity of a ferrite. The

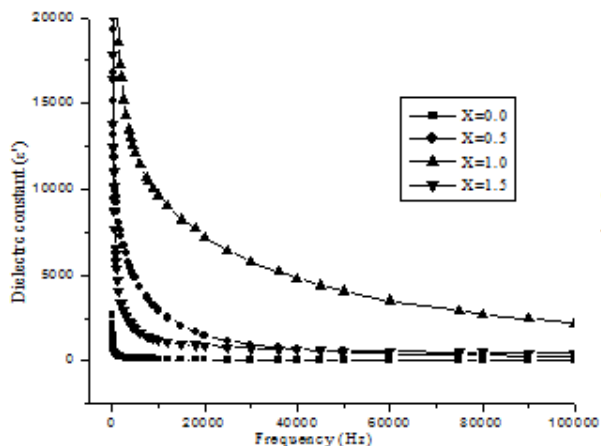


Fig.2 Frequency dependence of dielectric constant at room temperature

Since the number of the impurity atom is very limited, the hopping conduction mechanism plays a major role in the electric conduction and dielectric polarization process in these ferrites by electron hopping between Fe^{2+} and Fe^{3+} ions and hole transfer between Co^{+2} and Co^{+3} . It is well known that iron ions are distributed between both A and B sites. The Co^{+2} ion generally preferred octahedral sites, but when particles size reduced to nanodimensions, there is change in cations distribution and Co^{2+} occupy both octahedral (B) and tetrahedral (A) sites²⁴. Therefore the behavior of σ_{ac} , ϵ' and $\tan \delta$ with composition can be explained as follows: The substitution of TiCo ions up to

magnitude of electron exchanged between Fe^{2+} and Fe^{3+} ions depends upon concentration of Fe^{2+}/Fe^{3+} present on the crystallographically equivalent state in lattice i.e. on B-site. The Fe^{2+} ions concentration is a characteristic properties of a given ferrite material and its value depends upon various material synthesis parameters e.g. sintering temperature, cooling rate, type of annealing etc. The presence of Fe^{2+} ion which takes part in the electron exchange is responsible for the conduction and polarization. Thus, the highest value of ϵ' and σ_{ac} for compound $X=1.0$ may be attributed to the enhanced formation of Fe^{2+} ions. For the compounds with $X > 1.0$ the reduction in σ_{ac} is ascribed to decreasing octahedral ferric-ion concentration.

3.4 The Composition Dependence

The compositional dependence of the ac electrical conductivity (σ_{ac}), the dielectric constant (ϵ') and dielectric loss ($\tan \delta$) at 1kHz, 50kHz, 100kHz and 200kHz are illustrated in Fig. 5 - 7 respectively. It is shown that all the parameters increases with increase in "x" until they reach a maximum value at $X=1.0$, after which they start to decrease with further increase in TiCo content.

It stated that, the electric conduction in the studied sample is related mainly to the presence of the impurities and the hopping of charge carriers⁴.

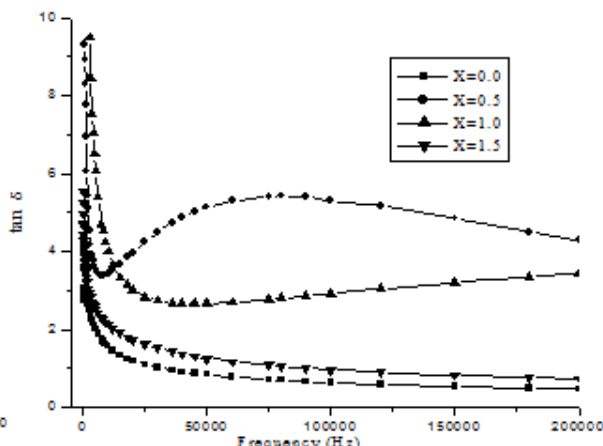
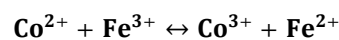


Fig.3 Frequency dependence of dielectric loss at room temperature

concentration $X=1.0$ increases the Co content at B sites which will increase the probability of hopping given by



Therefore conductivity increases up to $X=1.0$. However beyond $X=1.0$ Co ions may go to A site this will reduce the probability of hopping, consequently the conductivity decreases. The behavior of ϵ' and $\tan \delta$ can be explained on the basis of the assumption that the mechanism of dielectric polarization is similar to that of electrical conduction hence it is expected that behavior of ϵ' and $\tan \delta$ is similar to that of σ_{ac}

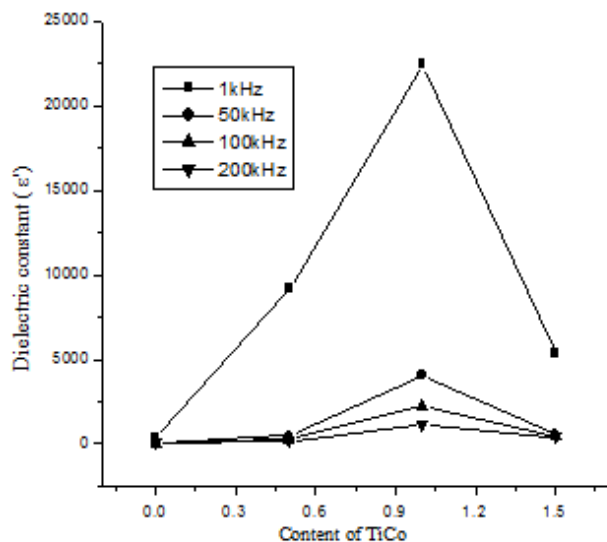


Fig.6 Composition dependence of dielectric constant

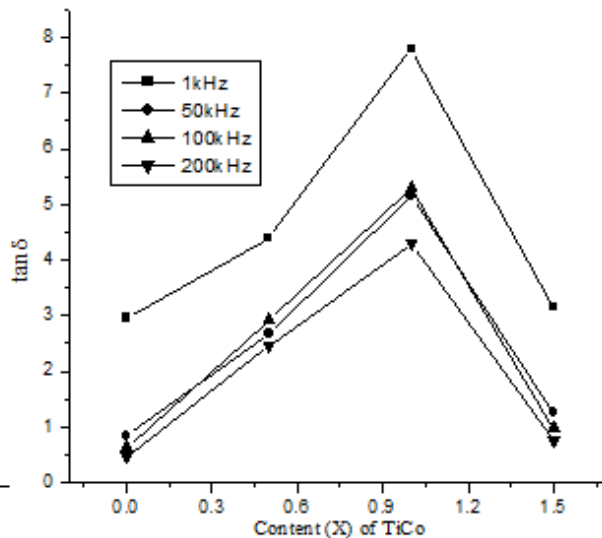


Fig.7 Frequency dependence of dielectric loss

4. Conclusions

A series of polycrystalline Sr_2NiZn Y-type nano hexaferrites substituted with TiCo having generic formula $\text{Sr}_2\text{NiZnFe}_{12-x}(\text{TiCo})_x\text{O}_{22}$ were successfully prepared by novel microwave assisted sol-gel auto combustion method. The X-ray diffraction pattern confirmed the formation of single Y-type hexaferrite phase in all prepared compounds. The crystallite size is found to be in range of 31 nm to 82 nm. The experimental density values were found to be much smaller than the X-ray density, indicating that prepared compounds are highly porous materials. The dielectric dispersion in ferrites has been explained on the basis of Maxwell-Wagner model. The highest value of ϵ' and σ_{ac} for compound $X=1.0$ may be attributed to the enhanced formation of Fe^{2+} ions.

References

- [1] Rosales M. I., Plata A. M., Nicho M. E., Brito A., and Ponce M.A... Castano V.M., J. Mater. Sci. **1995**, 30, 4446-4450
- [2] Guyot M, J. Magn. Magn. Mater. **1990**, 18, 925.
- [3] .Kwon H.J, J. Appl. Phys. **1994**, 75(10), 6109.
- [4] M.A. Ei Hiti, A.M. Abo Ei Ata, J. Magn. Magn. Mater. **1999**, 195, 667
- [5] Kony D.EI, Saafan S.A., Abo A, M, Ata EI, Egypt. J. Sol., **2000**, 23 (1), 137-146
- [6] Abo A, M, Ata EI, Hiti M.A EI., J. Phys. III France 1997, 7, 883.
- [7] George M, Nair SS, John AM, Joy PA, Anantharaman MR. J. Phys. D: Appl. phys. **2006**, 39, 900.
- [8] Gul IH, Abbasi AZ, Amin F, Rehman MA, Maqsood A., J. Magn. Magn. Mater. **2007**, 311: 494.
- [9] Kasap S O 2006 Principles of electronic materials and devices (New York: McGram- Hill)
- [10] Badwaik V., Badwaik D., Nanoti V., Rewatkar K., International Jour. of Knowledge Engineering, **2012**, 3, 1, 58-60.
- [11] Safaan S. A., Abo El Ata A.M., El Messeery M.S., J. Magn. Magn. Mater. **2007**, 302, 362-367.
- [12] Ganguly A, Mandal S K, Chaudhari S, Pal A K, J. Appl. Phys. **2001**, 90, 5652.
- [13] Koops C G Phys Rev.USA **1951**,83 121.
- [14] Shaik M A, Ballard S S, Chougule B K, J. Magn. Magn. Mater. **1996**, 152, 391.
- [15] Iwavchi K, J. Appl. Phys. **1971**, 10, 1520
- [16] Trivedi U N, Chhantbar M C, Modi K B, Johi H H, Indian J. Pure Appl. Phys. **2005**, 43, 688- 690.
- [17] Abo A.M Ata El., Attia S.M, J. Magn. Magn. Mater. **2003**, 257, 165-174
- [18] G.K. Joshi, S.A. Deshpande, A.Y. Khot, S.R. Sawant, Ind. J. Phys. A 61 (**1987**) 241
- [19] R.B. Jotania, R.V. Upadhyay, R.G. Kulkarni, IRRR Trans. Magn. 28 (**1992**) 1889
- [20] H. Patil, R. Upadhyay, N. Shamkuwar, R. Kulkarni, Solid State Commun. 81 (**1992**) 1011
- [21] M. Arshed, M. Butt, M. Siddique, A. Anwar, T. Abbas, H. Ahmed, Solid State Commun. 84 (**1992**) 717
- [22] E. Grandjean, A. Gerard, Solid State Commun. 25 (**1978**) 679
- [23] T.E. Whall, N. Salerno, Y.G. Proykova, V.A. Babers, Philos. Mag. Lett. B 53 (**1986**) 67
- [24] B.V. Shise, M.B. Dongar, S.A. Patil, S.R. Sawant, Phys. Rev. 122 (**1962**) 1447
- [25] J.S. Bijal, S. Phanijouban, D. Kothari, C. Prakash, P. Kishan, Solid State Commun. 83 (**1972**) 679
- [26] R. Bauminger, S.G. Cohen, A.M. Arinov, S. Ofer, E. Segal, Phys. Rev. 122 (**1962**) 1497
- [27] J. Smith, H.B.J. Wign, in: Ferrites, Cleaver-Hume Press, London, **1959**.